

1 Does size matter? The influence of size, load factor, range autonomy
2 and application type on the Life Cycle Assessment of current and
3 future trucks.

4 Romain Sacchi^{1*}, Christian Bauer¹, Brian L. Cox²

5 *1 = Technology Assessment group, Laboratory for Energy Systems Analysis, Paul Scherrer Institut, Villigen, Switzerland*

6 *2 = INFRAS, Bern, Switzerland*

7 **Corresponding author: email - romain.sacchi@psi.ch, telephone - +417 67 62 19 22, fax - +41 56 310 21 99*

8 Word count excluding Abstract, Keywords, Synopsis, Acknowledgement, Authors information, Funding sources
9 and References: approx. 6,900

10 Single figures: 4

11 Multi-part figures: 3

12 Tables: 0

13 Total word count: $6,900 + (4 * 300) + (3 * 600) = 9,900$

14 **Abstract**

15 The transparent, flexible and open-source Python library calculator_truck is introduced to perform the life cycle
16 assessment of a series of medium and heavy-duty trucks across different powertrain types, size classes, fuel
17 pathways and years in a European context. Unsurprisingly, greenhouse gas emissions per ton-km reduce as size
18 and load factor increase. By 2040, battery and fuel cell electric trucks appear to be promising options to reduce
19 greenhouse gas emissions per ton-km on long distance segments, even where the required range autonomy is high.
20 This requires that various conditions are met, such as improvements at the energy storage level and a drastic
21 reduction of the carbon intensity of the electricity used for battery charging and hydrogen production. Meanwhile,
22 these options may be considered for urban and regional applications, where they have a competitive advantage
23 thanks to their superior engine efficiency. Finally, these alternative options will have to compete against more
24 mature combustion-based technologies which, despite lower drivetrain efficiencies, are expected to reduce their
25 exhaust emissions via engine improvements, hybridization of their powertrain as well as the use of biomass-based
26 and synthetic fuels.

27 **Keywords**

28 battery, fuel cell, electric, open-source, freight, transport, tank-to-wheel, prospective

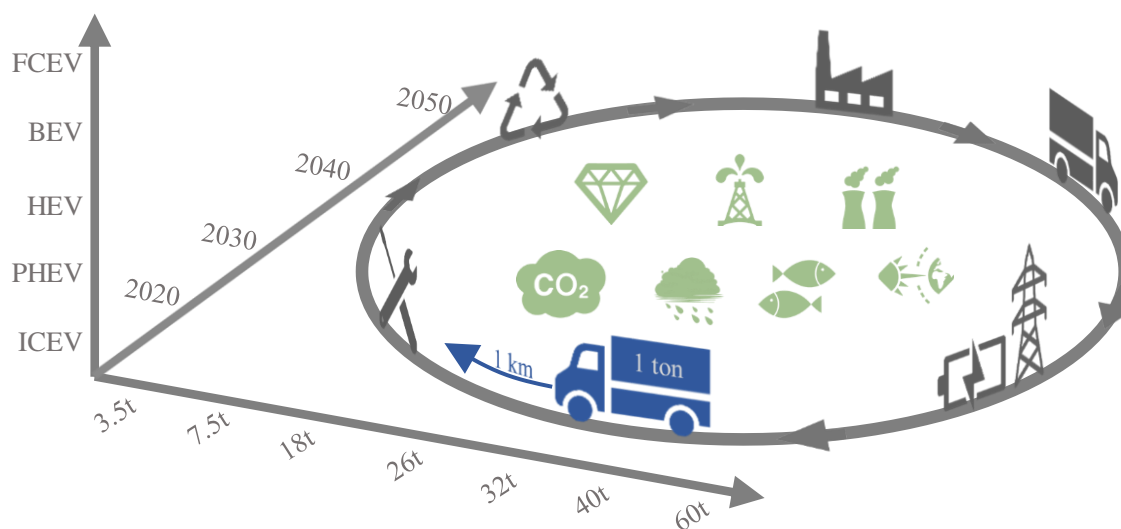
29 Acronyms

ICEV-d	Internal combustion engine vehicle, powered by diesel fuel
ICEV-g	Internal combustion engine vehicle, powered by compressed gas
HEV-d	Hybrid engine vehicle, powered by diesel fuel
PHEV-d	Plug-in hybrid engine vehicle, powered by diesel fuel and electricity
BEV	Battery electric vehicle
FCEV	Fuel cell electric vehicle
CNG	Compressed natural gas
MGV	Medium goods vehicle
LGV	Large goods vehicle

30 Synopsis

31 Battery and fuel cell trucks can reduce GHG emissions from road transport substantially, but the actual reduction
32 depends on developments in other sectors.

33 Abstract art



34

35 1 Introduction

36 Mitigating climate change impacts and keeping the atmospheric temperature increase under 2°C by 2100
37 (compared to 1990 levels) requires a substantial and fast reduction of anthropogenic greenhouse gas (GHG)

38 emissions in all economic sectors ¹. Road transport is an important source of GHG emissions worldwide: in
39 2018, heavy duty vehicles (HDV) released 1,770 Mt of CO₂ via their exhaust emissions². It represents more than
40 5% of the energy-related CO₂ emissions emitted that year ³. Emissions from these vehicles exhibited an annual
41 growth rate of 2.6% since the year 2000 ². In the European Union (EU), CO₂ emissions from HDV currently
42 represent 6% of total CO₂ emissions and 25% of total road transport CO₂ emissions. To reduce these emissions
43 and align with the long-term strategy of carbon neutrality in 2050, the EU has released a regulation with
44 mandatory goals: specific CO₂ emissions of new HDV shall be reduced by 15% and 30% in 2025 and 2030,
45 respectively, compared to 2020 ⁴. These goals might be achievable using conventional diesel trucks with a
46 higher energy efficiency, but in the long term, “zero-emission” vehicles such as battery electric (BEV) and fuel
47 cell electric vehicles (FCEV) will be required.

48 However, these so-called “zero-emission” vehicles only exhibit zero GHG emissions during vehicle operation.
49 Indeed, substantial GHG emissions are associated to the production of these vehicles as well as the fuel supply.
50 This has been shown for passenger vehicles in the past ⁵⁻¹³. There is now sufficient evidence that BEV and
51 FCEV passenger vehicles can reduce life cycle GHG emissions if batteries are charged with low-carbon
52 electricity and hydrogen production is associated with low GHG emissions. However, because HDV differ from
53 passenger cars in terms of specifications, operational requirements and function, the environmental life cycle
54 performance of HDV might differ significantly.

55 Therefore, a thorough analysis is required for HDV as well. Regarding medium (MGV) and large (LGV) goods
56 vehicles, literature on their life cycle environmental performance is scarce and limited in terms of temporal,
57 technological and application scope. Several studies have evaluated the life cycle environmental burden of
58 (current) BEV trucks in comparison with non-electric technologies ¹⁴⁻¹⁸. But the scope of these studies remained
59 limited: some did not consider all size classes ^{14,15,18} or all powertrain types¹⁷, other limited the supply of
60 hydrogen to one pathway ¹⁶, while none included future perspectives. Additionally, the important relation
61 between payload and energy storage requirements for BEV trucks, as demonstrated by Sripad and
62 Viswanathan¹⁹, seems largely ignored.

63 This overview shows that a comprehensive life cycle-based comparison of the environmental performance of
64 trucks across drivetrains, fuel pathways and size classes is missing. Such evaluation should consider potential
65 future development, since it is expected that BEV and FCEV will profit more substantially from future
66 developments than mature conventional drivetrains.

67 This paper addresses these research gaps and presents *calculator_truck*, an open-source LCA model to analyze
68 the life cycle environmental performance of MGV and LGV with an unprecedented scope, flexibility,
69 transparency and level of detail. The model covers:

- 70 • Six powertrain technologies: diesel, diesel-hybrid, plugin diesel-hybrid, compressed gas, fuel cell and
71 battery electric powertrains.
- 72 • Seven size classes (referring to the gross vehicle weight): 3.5-ton delivery trucks, 7.5-ton, 18-ton and
73 26-ton rigid trucks, as well as 32-ton, 40-ton and 60-ton articulated trucks. MGV refers to vehicles with
74 a gross weight between 3.5 and 26 tons, while LGV are vehicles with a gross weight above 26 tons.
- 75 • Three application types: urban and regional deliveries as well as long haul, associated to a range
76 autonomy of 150, 400 and 800 km respectively.
- 77 • Over a period of 50 years, defined by six points in time (from 2000 to 2050 by 10-year steps). FCEV
78 and BEV trucks are not modeled before 2020.
- 79 • With over twelve different fuel pathways: diesel, biodiesel, natural gas, bio-methane, electricity,
80 hydrogen, synthetic fuels, etc.

81 This paper highlights the influence of size, range autonomy, technological improvement and duty cycle on the
82 respective environmental performance of powertrain technologies and specific fuel chains.

83 2 Method

84 LCA consists in quantifying the release of environmentally harmful emissions of a product or service along each
85 of the relevant phases of its life cycle. In the case of trucks, this includes the manufacture of their components,
86 their assembly, the use and maintenance of the trucks as well as their disposal. These emissions are expressed in
87 reference to a functional unit to offer a common basis for comparison between trucks of different technologies
88 and sizes. The functional unit typically used to compare trucks is the transport of 1 ton of cargo over 1 km.
89 These emissions are then characterized against indicators that reflect the burden and damage borne by mid-
90 (e.g., Global Warming) and endpoint (e.g., Human health) recipients, respectively, via cause-effect pathways
91 (e.g., from the emission of a greenhouse gas to the radiative forcing of the atmosphere). The process ranging
92 from emissions inventory to impacts characterization is governed by a series of international standards, namely
93 ISO 14040²⁰ and ISO 14044²¹.

94 This study introduces *calculator_truck*, which is an open-source Python library that allows to perform LCA of
95 MGV and LGV under different future energy scenarios. Its source code is hosted on an online public
96 repository¹. This ensures that the code, algorithms and assumptions behind the model can be viewed, criticized
97 and improved by the community at large. A notebook using this library is included in the Supplementary
98 Information (SI) to ensure that all the results and figures presented in this study are reproducible, provided the
99 same version of the library is used². This library operates similarly to *calculator*, another Python library for
100 modeling life cycle impacts of passenger cars ⁶. It mainly revolves around the following 3-step workflow:

- 101 1. Arrays that contain input parameters are loaded. The spectrum of input parameters is wide and listed in
102 Table 1 of the SI. It includes, for example: parameters defining the efficiency of the engine, the mass of
103 the battery charger, but also the energy density of battery cells. The arrays are three dimensional as the
104 input parameters are defined across powertrains, size classes and years.
- 105 2. An algorithm iterates between components, dimensions and masses and the energy consumption of the
106 vehicles, to find technically feasible solutions given a set of constraints. The set of constraints includes,
107 among others, the minimum range autonomy for BEV or the CO₂ reduction targets for internal
108 combustion engine vehicles (ICEV). At this stage, CO₂ and other exhaust and non-exhaust emissions
109 (i.e., hot pollutants, noise) are calculated based on the selected driving cycle and the associated fuel
110 consumption.
- 111 3. Once the vehicles are modeled, the total material and energy requirement for each truck is calculated.
112 The inventories are characterized against midpoint (e.g., Climate change) or endpoint (e.g., Human
113 health impacts) environmental indicators.

114 Each of these three points are discussed in the next sections. The validation of the vehicle models against
115 literature data and existing vehicles is included in the SI.

116 2.1 Input parameters definition

117 Values for input parameters are stored for all vehicles across three dimensions: powertrain type, size class and
118 year. Most of the values for these parameters are given with uncertainty distributions, making it possible to
119 perform error propagation analyses. *calculator_truck* uses over 70 parameters to build 252 unique truck models
120 (6 powertrain types, 7 size classes, at 6 points in time). Table 1 in the SI lists these parameters and whether their

¹ https://github.com/romainsacchi/calculator_truck

² Version 0.0.7 at the time of writing

121 values change across powertrain types, size classes and years. Sources, values, uncertainty distributions and
122 descriptions for these parameters are also included as a spreadsheet in the SI.

123 2.2 Sizing, energy consumption and emissions of vehicles

124 The next subsections describe how the vehicles are dimensioned and how the fuel consumption and emissions
125 are calculated.

126 2.2.1 Mass distribution

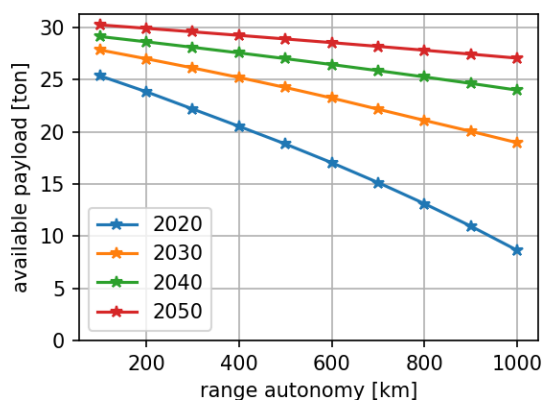
127 First, the model brings together the components common to all powertrains. These include the chassis, the
128 cabin, the onboard electronics, the suspension system, the brake system and the wheels and tires. Such
129 components for diesel trucks across size classes are listed in Table 2 of the SI. The weight composition by
130 components are the result of cross-checking several sources, as indicated in that same table. Most of the values
131 are based on a 12-ton and 40-ton truck from ^{22,23}, further adapted to other size classes for which curb and
132 payload masses are known from the database Car2db ²⁴. Second, powertrain-specific components are added,
133 such as the internal combustion engine and fuel tank for ICEV-d and ICEV-g, an electric motor with batteries
134 for BEV trucks, or with a fuel cell stack and a hydrogen tank for FCEV trucks. For these components, the 40-ton
135 truck model of Wolff et al. ²³ is principally used. Across time, it is assumed that such composition does not
136 change. However, a light-weighting factor is applied to the sub-components of the chassis system as listed in
137 Table 2 of the SI, according to ²², going from 2 and 5% in 2020, to 28 and 30% in 2050 for MGV and LGV
138 respectively, compared to 2010. To that effect, this weight reduction over time is modelled as steel being
139 substituted by aluminium²⁵.

140 The sum of the mass of the vehicle components corresponds to the curb mass. The available payload is
141 calculated as the gross vehicle mass, to which the curb mass, the fuel mass and the driver mass are subtracted.
142 The actual cargo mass is the product of the available payload and the load factor. The sum of the curb mass, the
143 fuel mass, the driver's mass and the cargo mass constitute the driving mass.

144 Because some of the vehicle components are scaled on the energy consumption of the vehicle (such as the
145 engine, but also the batteries), and because the energy consumption of a vehicle is affected by its driving mass,
146 those are defined iteratively until their values converge (i.e., until they do not change significantly between two
147 iterations).

148 2.2.2 Sizing of energy storage components

149 The sizing of some components also depends on the required range autonomy of the vehicle – the distance it
 150 must be able to drive on a single tank filling/battery charging. This is particularly relevant for BEV trucks. The
 151 tank-to-wheel energy consumption (see next section) and the range autonomy are determinant to the battery
 152 capacity. The mass of the batteries is primarily determined by the energy density of the cells. As the driving
 153 range increases, the batteries “eat away” some of the payload capacity. If the vehicle curb mass reaches the
 154 vehicle gross mass, the payload capacity becomes inexistent and the vehicle cannot be considered further. For
 155 example, Figure 1 shows the available payload function of the required range autonomy for a 40-ton BEV truck,
 156 from 2020 to 2050. Expected improvement of the energy density of battery cells over time, going from 0.2
 157 kWh/kg today ²⁶, and up to 0.5 kWh/kg in 2050 ²⁷, is the primary enabler for increasing the available payload
 158 given a required range autonomy – as well as other improvements that indirectly reduce the curb mass. By
 159 default, the required range autonomies of 150, 400 and 800 km are respectively set for the three driving cycles
 160 available, namely “Urban delivery”, “Regional delivery” and “Long haul”.



161

162 Figure 1 Available payload as a function of the range autonomy for a 40-ton BEV truck.

163 2.2.3 Fuel and electricity supply

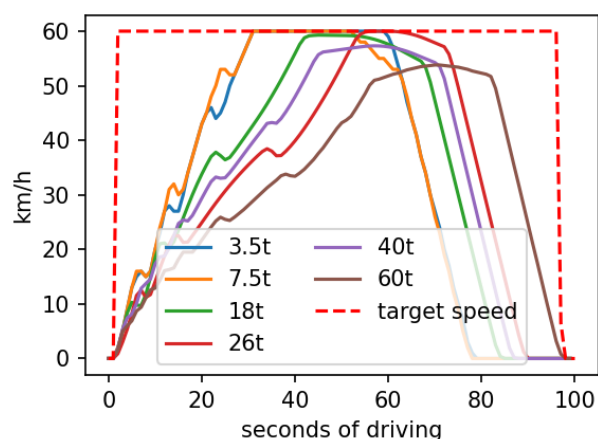
164 Over twelve different fuel pathways are available to power the vehicles. They include traditional fuels like
 165 diesel, natural gas and biofuels, but also fuels from emerging technologies like hydrogen from reforming of bio-
 166 methane or wood gasification (with and without carbon capture and storage)^{28,29} or synthetic methane from
 167 hydrogen and carbon dioxide from direct air capture³⁰. The fuels are listed in Table 3 of the SI. Custom fuel
 168 blends can be specified. Some fuel blends can contain a significant amount of alternative fuel, which
 169 characteristics can also affect the required energy storage capacity. For example, an extensive use of biodiesel,

170 which has a lower net calorific value than conventional diesel, leads to filling the truck tank with a larger
171 amount of fuel to maintain the required range autonomy. This increases the driving mass of the vehicle and its
172 energy consumption.

173 For vehicles that require electricity directly (e.g., BEV, for battery charging) or indirectly (e.g., FCEV, to supply
174 hydrogen via electrolysis), the electricity mix is either user-defined or calculated based on the country of use.
175 The former option allows to conduct analyses using a specific electricity technology (e.g., wind power only). In
176 the second option, the electricity mix used is a result of the averaged projected electricity mixes over the period
177 of use of the vehicle (e.g., from 2020 to 2032, if the vehicle is first used in 2020 and has an expected lifetime of
178 12 years) in the specified country. This tends to result in “greener” electricity mixes than simply using the
179 electricity mix of the first year of use. Indeed, projected national electricity grid developments (often
180 synonymous with expanding renewable energy sources) are accounted for. *calculator_truck* includes gross
181 electricity mixes for ninety countries from 2000 to 2050. Projections for European, African and remaining
182 countries are from ³¹, ³² and ³³, respectively.

183 2.2.4 Tank-to-wheel energy consumption

184 When a preliminary value is given to the driving mass, the different resistances the vehicle must overcome are
185 calculated for each second of the driving cycle. As their names suggest, the three driving cycles available
186 represent different types of applications. They define the target speed levels for every second of driving and are
187 extracted from the VECTO software ³⁴. The actual speed profiles considering the vehicles specifications (i.e.,
188 driving mass, engine power, gearbox, etc.) for the first hundred seconds of the “Long haul” driving cycle are
189 depicted in Figure 2, based on a simulation using the VECTO software. Intuitively, heavier vehicles need more
190 time to reach the target speed. There is however an interesting aspect also highlighted: the 40-ton and 60-ton
191 vehicles do not simply have time to reach the target speed as they already need to decelerate to come to a stop
192 by second 90 and 100, respectively. Lighter vehicles, on the other end, tend to have steeper accelerations and
193 start decelerating (or braking) later comparatively. This trend is observed on most of the driving cycle duration
194 and mostly on driving cycles with frequent stops. It results in heavier vehicles reaching, on average, lower speed
195 levels with narrower fluctuations in speed levels than lighter vehicles.



196

197 Figure 2 Speed profiles per second of driving for the first one hundred seconds of the “Long haul” driving cycle.

198

199 For each second of the driving cycle, the various types of resistance encountered by the vehicles are calculated.

200 This allows to obtain the amount of power that should be transmitted at the wheels. This is then compared to the

201 results obtained from the VECTO simulations, using similar trucks specifications. Finally, the tank-to-wheel

202 energy requirement should be calculated. Here, VECTO uses a complex model considering gearbox and engine

203 torque maps, where the efficiency of those components varies according to the gear used, but also the speed and

204 torque to deliver. While replicating such model would be outside of the scope of this study, a simpler approach

205 is adopted. The efficiency of the engine and the transmission is approximated based on the relative power load

206 required. This reflects an increase in efficiency for both the engine and the transmission as the drivetrain

207 operates closer to its maximum rated power output. It also allows to consider the effect of engine downsizing.

208 The details of such modeling and the calibration and validation against VECTO simulations are detailed in the

209 Section 2.3 of the SI. The tank-to-wheel energy consumption calculated by *calculator_truck* and VECTO with

210 trucks of similar specifications do not differ by more than 1% on all driving cycles. Hybrid diesel vehicles (i.e.,

211 HEV-d and PHEV-d), for which part of the combustion engine power has been re-allocated to an electric motor,

212 reach higher efficiency levels as the engine operates more often at relatively higher power load. They also have

213 the advantage of being able to recuperate a part of the energy spent braking or decelerating thanks to their

214 electric motor, if the driving cycle chosen permits it.

215 VECTO does not come with engine maps for CNG engines. Hence, current efficiencies for CNG engines are set

216 to be 19% lower than what is obtained from the calibration of ICEV-d trucks, corresponding to the performance

217 of a spark-ignition CNG engine, according to³⁵. By 2030, the engine is assumed to be of compression-ignition

218 type to achieve better performances. It reflects the use of a dual CNG-diesel fuel injection system, which
219 reduces the relative difference in thermal efficiency compared to a diesel engine to 14%, as reported by ³⁵. After
220 2030, the efficiency of the CNG engine converges with that of a diesel engine to reach equivalent performances
221 by 2050, as also suggested by ³⁵.

222 In the absence of electric motor specifications in VECTO, such calibration could neither be extended to BEV or
223 FCEV powertrains. Instead, literature data from electric and fuel cell vehicles – see Tables 6 and 7 of the SI – is
224 used to approximate the engine and transmission efficiency rates of those powertrains. Like HEV-d and PHEV-
225 d, FCEV and BEV trucks can recuperate a fraction of the braking energy during deceleration or downhill
226 sections of the driving cycle.

227 In a comparison between trucks from 1994 and 2015, Transport & Environment ³⁶ demonstrates that the fuel
228 efficiency of North American and European trucks over that period remained unchanged. Engine efficiencies
229 did not markedly increase due to additional emissions-limiting measures which led manufacturers to increase
230 the engine power, and thereby the fuel consumption. The curb mass of the vehicles also did not decrease. In fact,
231 it seems to have slightly increased due to additional safety equipment. Default efficiency values reflect that past
232 development.

233 As for the projected developments over the period 2021-2050 for diesel and compressed natural gas-based
234 powertrains, CO₂ targets for trucks as implemented by the European Union ³⁷ are used by default. These targets
235 correspond to a 15% and 30% reduction of CO₂ exhaust emissions by 2025 and 2030 respectively, compared to
236 2020, on a fleet basis. While it is not entirely correct to use fleet-based targets on single vehicle technologies, it
237 is unlikely that “zero emissions” vehicles will represent a significant share of any fleet by 2030. Hence, diesel
238 and compressed natural gas trucks will still have to substantially reduce their exhaust emissions down by a
239 factor close to the mentioned target. In their 2018 report, ICCT forecasts a number of energy efficiency
240 improvements for diesel trucks at the engine level by 2030, including waste heat recovery, engine downsizing,
241 etc., to comply with future regulations on energy efficiency ³⁸. In *calculator_truck*, a similar approach is used
242 by increasingly hybridizing the powertrain to reduce the size of the combustion engine, as it is being
243 compensated by an electric motor. It results in additional recuperated energy – only if the driving cycle permits
244 it – and the combustion engine to operate less often, but at a higher power load, where its thermal efficiency is
245 higher. *calculator_truck* iteratively increases the hybridization rate of the powertrains until they comply with
246 the defined emission reduction targets. If the driving cycle does not allow for substantial energy recuperation,

247 energy efficiency gains through the hybridization of the powertrain will be limited. If the energy efficiency
248 gains are insufficient, the vehicles are declared “non-compliant” but their results are still calculated. The user
249 has the possibility to change these emission targets to reflect other policies.

250 2.2.5 Fuel-related exhaust emissions

251 Carbon dioxide emissions that result from the combustion of liquid and gaseous fuels are calculated based on
252 the tank-to-wheel energy consumption of the vehicle, the net calorific value of the fuel blend as well as its CO₂
253 emission factor. The combustion of biofuels and synthetic fuels also leads to CO₂ emissions. They are though
254 compensated by the CO₂ uptake during the fuel preparation (i.e., biomass growth for biofuels, or direct air
255 capture for synthetic fuels). Several heavy metals are also emitted because of burning conventional diesel and
256 are calculated using the emission factors expressed in kg/kg diesel as reported in ³⁹.

257 Sulfur dioxide emissions are also calculated based on fuel consumption. A varying sulfur content in the diesel
258 fuel is considered across geographies and time. Time series for the sulfur content in fuels for a limited number
259 of countries (i.e., Austria, Switzerland, France, Germany and Sweden) are extracted from the HBEFA 4.1
260 database ⁴⁰, while ⁴¹ provides current sulfur content for over 190 other countries. Additionally, European
261 countries for which specific time series are not available are assumed to follow the European regulations on
262 sulfur content in on-road diesel fuel (from 2,000 ppm in 1994 down to 10 ppm today). Finally, it is assumed that
263 countries that have a sulfur content above 50 ppm today will converge towards a concentration of 50 ppm by
264 2050, as recent developments seem to suggest ⁴². Figure 7 of the SI shows a map of sulfur concentration values
265 in on-road diesel fuel considered in 2020.

266 Finally, pump-to-tank leaks when filling with gaseous fuels are also considered. They are accounted for as a
267 fraction of the fuel input, with a median value of 0.4%, as reported by ³⁵, being directly emitted as methane.

268 2.2.6 Emissions of regulated substances

269 Several other emissions, which also correlate with the fuel consumption, occur during the use phase of the
270 vehicle. It is the case of hot pollutants such as CO, NO_x, CH₄, etc. These substances, which are regulated by
271 European emission standards, are calculated based on the fuel consumption of the vehicle, for each second of
272 the driving cycle. A linear regression fit is modelled across emissions factors supplied by the HBEFA database
273 4.1 ⁴⁰, for different fuel consumption levels, EURO emission standards and traffic situations. Additionally, a few
274 compounds are derived as a fraction of total non-methane volatile organic compound emissions, such as

275 benzene, toluene, xylene, formaldehyde and acetaldehyde ³⁹. The correlation used between emissions factors
276 and fuel consumption for different emission standards and fuel types is depicted in section 2.6 of the SI.
277 Emission factors for future ICEV-d and ICEV-g vehicles are not known and are assumed to remain at the level
278 of 2020 (i.e., EURO VI). Potential hybridization of their powertrains in the future, where an electric motor
279 assists the internal combustion engine, helps reduce these emissions.

280 Furthermore, different environments of use are identified within each driving cycle to differentiate calculated
281 emissions by compartment of emissions, namely urban, suburban and rural. The respective shares of emissions
282 by compartment for each driving cycle are specified in Table 4 of section 2.5 of the SI. Distinct characterization
283 factors – depending on the Life Cycle Impact Assessment (LCIA) method applied are used for assessing their
284 impacts regarding. It is the case, for example, with impacts on the human respiratory system, as different
285 characterization factors for emissions are used for urban, suburban and rural compartments, reflecting
286 differences in population density.

287 2.2.7 Non-exhaust emissions

288 Several non-exhaust emissions are also considered, namely abrasion particles from tires, brakes and road wear,
289 but also noise emissions, from tire rolling and propulsion.

290 2.2.7.1 Abrasion particles

291 Based on the Tier-2 methodology presented in ⁴³, brakes, tires and road wear emissions are calculated
292 considering the driving cycle, number of axles and the load factor of the vehicle. Additionally, based on the
293 evaluation report of the American Fuel Cell Bus project ⁴⁴, where the maintenance costs of 5 CNG buses were
294 compared to those of 4 FCEV buses over 18 months in 2011, the cost in brake part replacement for FCEV buses
295 were only 10% of that of CNG trucks. Such difference is also used by default in this study to adjust brake wear
296 particle emissions for trucks equipped with an electric motor – the user can however easily modify this
297 assumption.

298 2.2.7.2 Noise emissions

299 Noise emissions are calculated according to the CNOSSOS model ⁴⁵. First, sound power, in A-weighted
300 decibels, is calculated for each second of the driving cycle, with tire rolling and propulsion noise coefficients for
301 medium and heavy-duty vehicles and correction coefficients for electric powertrains ⁴⁶. Propulsion noise usually
302 dominates up to 50 km/h. Above that speed, rolling noise becomes predominant, regardless of the powertrain.

303 The sum of noise power over time divided by the distance of the driving cycle results in noise energy (joules)
304 per km driven, which are then converted in Person-Pascal-second. As with hot pollutant emissions, different
305 emission compartments are identified for each driving cycle (i.e., urban, suburban and rural), as environment-
306 specific characterization factors (from Person-Pascal-second to Disability-Adjusted Life Year) are used to assess
307 the impact of noise energy on human health, according to ⁴⁷.

308 2.3 Material and energy inventory

309 The vehicle components, their size and mass and the vehicle energy consumption are part of the foreground
310 aspect of the model. The supply of energy, materials and services needed to support the different life cycle
311 phases of the vehicle are part of the background aspect of the model. Foreground and background aspects of the
312 model are approached differently.

313 2.3.1 Foreground inventory

314 Table 5 of the SI lists the different component datasets used as well as their sources. Most of these components
315 rely on the supply of material, energy and services, provided by the background inventory databases presented
316 in the next section.

317 2.3.2 Background inventory

318 Foreground inventories link to background inventory databases. Background inventory databases are created
319 using *rmnd_lca* ⁴⁸, a Python library which integrates the outputs of the global Integrated Assessment Model
320 REMIND ⁴⁹ into the LCA database ecoinvent v.3.7 (system model “allocation, cut-off by classification”) ⁵⁰.
321 Variants of the ecoinvent database have been created for the years 2000 to 2050, by 10-year steps, under
322 different REMIND energy scenarios defined by Shared Socioeconomic Pathways (SSP). Across time within a
323 same energy scenario, the energy efficiency and emissions of power plants in the database are adjusted, as well
324 as electricity supply markets. Across energy scenarios, the presence of emerging technologies, notably Carbon
325 Capture and Storage (CCS), is introduced to varying degrees. Variants of the ecoinvent database available in
326 *calculator_truck* are created based on different energy scenarios³. Results displayed in the next section use the
327 *baseline* energy scenario of “SSP2” – the reader can refer to ⁵¹ for more information on SSP. This is a
328 conservative scenario that projects cumulative GHG emissions to reach 5,000 Gt globally by 2100

³ A description of available energy scenarios available in the *rmnd-lca* library is available:
https://github.com/romainsacchi/rmnd-lca/blob/master/rmnd_lca/data/remind_output_files/description.md

329 (corresponding to an increase in atmospheric temperature of 4 degrees Celsius). Modifications at the power
330 generation level and its supplying markets affect all the activities in the database and is of great relevance for the
331 supply of electricity, but also steel, aluminum and other energy-intensive materials for prospective analysis.

332 2.3.3 Impact assessment

333 Foreground and background inventories values are stored in a three-dimension array A , which dimensions are
334 supplying activities, consuming activities and iterations (which length equals 1 in the case of a simple analysis,
335 or the number of iterations in the case of a Monte Carlo or sensitivity analysis). The total requirements in terms
336 of material and energy from each supplying activities, represented by a scaling factor x , are obtained given a
337 demand vector f (i.e., 1 ton-km from a specific vehicle) so that $Ax = f$.

338 Another multi-dimensional array B , which contains pre-calculated values of ecoinvent activities for different
339 mid- and endpoint indicators for different years and REMIND energy scenarios, is multiplied with x to obtain
340 the environmental impacts associated to the functional unit.

341 The available mid- and endpoint impact assessment indicators are part of Recipe 2008⁵² as well as ILCD 2018
342⁵³. The library also allows to export inventories in different formats, to be reused in LCA software such as
343 Brightway2⁵⁴ and Simapro⁵⁵ where other indicators are available.

344 For this analysis, results are shown using the Global Warming Potential indicator based on IPCC's 2013
345 characterization factors⁵⁶, expressed in kg CO₂-eq. with a time horizon of 100 years. As mentioned earlier, the
346 *baseline* energy scenario of the Shared Socioeconomic Pathway SSP2 is used for projections.

347 3 Results

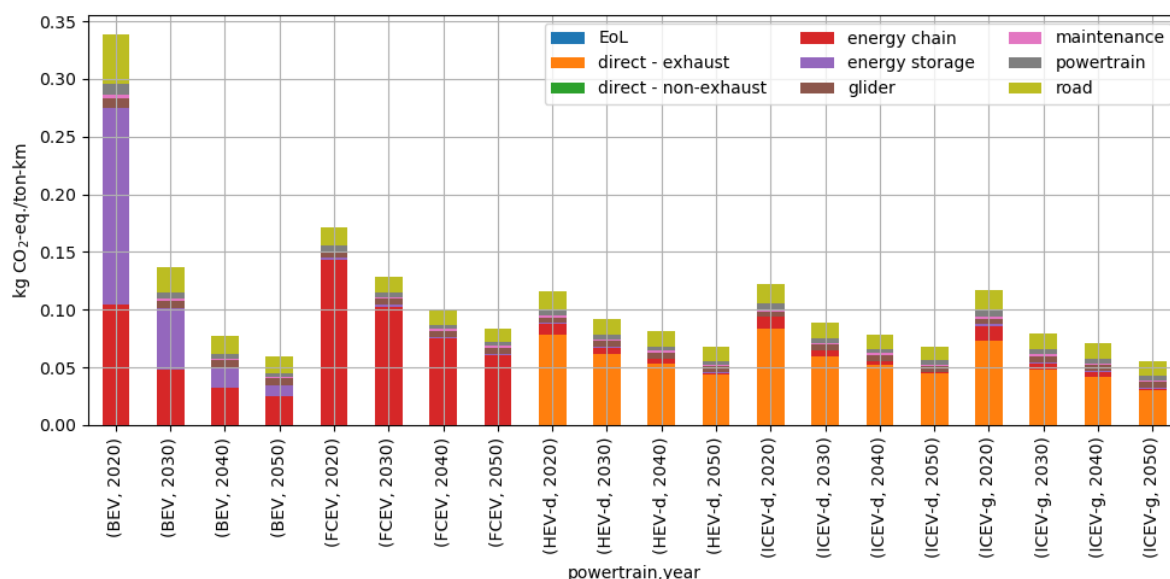
348 This section presents comparative results across powertrains, size classes and applications. While
349 *calculator_truck* has a wide catalogue of impact assessment indicators and energy scenarios, the results
350 presented here use a baseline energy scenario with the Global Warming Potential indicator. Additionally, the
351 various calculated trucks specifications (i.e., loading factor, tank-to-wheel efficiency, fuel consumption) the
352 results are based upon, are detailed in sections 4.1 to 4.3 of the SI document.

353 3.1 Comparison across powertrains and duty cycles

354 Figure 3 compares the GHG emissions per ton-km of a 40-ton vehicle across powertrain types and years, for the
355 “Long haul” driving cycle. Vehicles for the years 2000 and 2010 are left out to avoid displaying too much
356 information. Similar figures for the “Urban delivery” and “Regional delivery” driving cycles are included in the
357 SI – see Figure 12 of the SI. This analysis uses the yearly mileage-weighted electricity consumption mix in the
358 European Union given by the baseline REMIND projection for SSP2 over the lifetime of the trucks (e.g., from
359 2020 to 2032 for vehicles of the year 2020, from 2030 to 2042 for vehicles of the year 2030, etc.) to charge
360 batteries and produce hydrogen. For vehicles of the year 2020, it consists of 10% hydro power, 15% nuclear
361 power, 17% natural gas power, 25% from waste incineration, 5% photovoltaic power, 10% wind power, 3%
362 biomass-based power, 13% coal-based power and 1% from fuel oil, for an overall carbon intensity of 255 g
363 CO₂-eq./kWh. The carbon intensity of the vehicles of the years 2030, 2040 and 2050 is 233, 225 and 221 g CO₂-
364 eq./kWh respectively.

365 Across driving cycles, the urban context of use (as reflected by the “Urban delivery” driving cycle – see Figure
366 12.a of the SI) seems to be more energy-demanding than when driving at a constant, albeit higher speed level, as
367 reflected by the “Long haul” driving cycle, as shown here in Figure 3. This is an opportunity for BEV trucks
368 which are generally more energy efficient. For urban applications with a limited range autonomy, BEV trucks
369 appear to become a viable and competing option in terms of life cycle GHG emissions per ton-km as soon as
370 2020. On the other hand, in a long-hauling scenario with a larger range autonomy required, there is a higher
371 impact associated to energy storage for BEV and the effect of its mass on the motive energy requirement, which
372 do not manage to be among the preferred options before 2040, as shown in Figure 3. ICEV-d trucks, despite
373 reducing their on-road GHG emission by 15% between 2020 and 2030, do not manage to keep up with fully
374 electrified powertrains on the long-term (i.e., after 2030). Despite a lower CO₂ emission factor for compressed
375 natural gas, *current* ICEV-g trucks are penalized by a relatively inefficient spark ignition engine together with
376 methane emissions along the fuel supply chain. By 2030, the adoption of compression ignition engines should
377 help ICEV-g trucks to align with the GHG emissions of ICEV-d trucks. However, it is not before the
378 performances of gas engines fully align with those of diesel engines in 2050 that ICEV-g trucks will offer a
379 clear benefit in terms of GHG emissions. Finally, FCEV trucks, running on hydrogen produced by electrolysis,
380 have the advantage of having an electrified powertrain with a reduced mass for energy storage relative to BEV
381 trucks. Yet, in this scenario, they do not manage to outcompete ICEV-d and ICEV-g trucks due to their

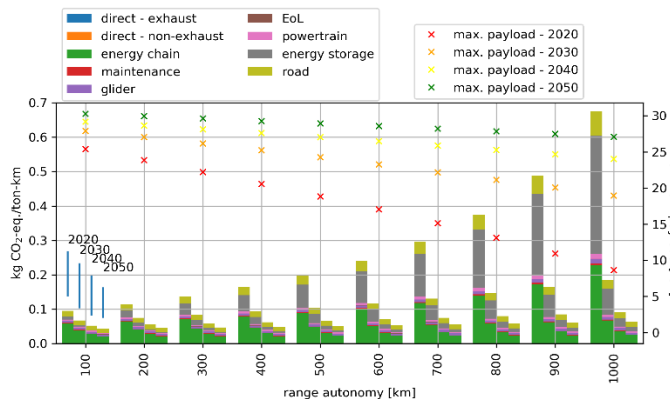
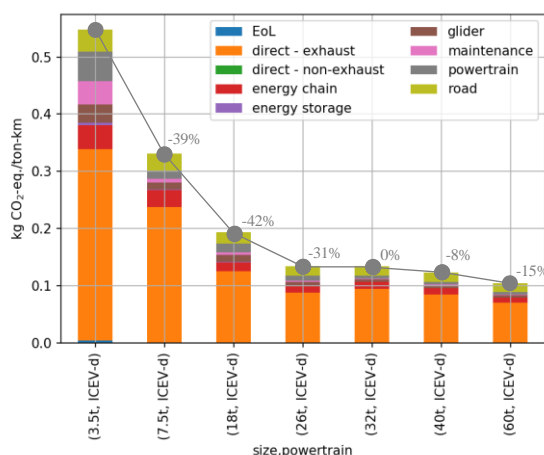
382 relatively inefficient energy chain combined with an electricity still too GHG-intensive on average by 2050 (i.e.,
 383 221 g CO₂-eq./kWh).



384
 385 Figure 3 Per ton-km GHG emissions comparison across powertrains and years for 40-ton trucks, for the "Long
 386 haul" driving cycle, with a range autonomy of 800 km. Fuel for ICEV-g: compressed natural gas. Fuel for
 387 FCEV: electrolysis-based hydrogen.

388 3.2 Importance of size class, driving range and load factor

389 Figure 4.a shows clear economies of scale despite lower size vehicles benefitting from a higher load factor. This
 390 is easily explained by the decreasing payload-to-curb mass ratio, calculated as ranging from 1.06 ton of curb
 391 mass per ton of payload for a 3.5-ton truck, down to 0.57 for a 60-ton truck. Figure 4.b shows the influence of
 392 the energy density of battery cells on the payload capacity of a 40-ton BEV truck as a function of the range
 393 autonomy. As the range autonomy increases, so does the battery mass. This leads to impacts evolving in a more
 394 than proportional manner as the overall impacts are normalized by the cargo mass transported, which itself
 395 converges towards zero (as it is increasingly being replaced by the battery mass). While this effect has a very
 396 substantial impact on the results today with the current battery technology, the expected improvements are
 397 significant by 2050. However, they are only realized if the energy density of battery cells does reach 0.5 kWh/kg
 398 cell by 2050. As of today, BEV trucks do not seem to be suitable for long-hauling operations.



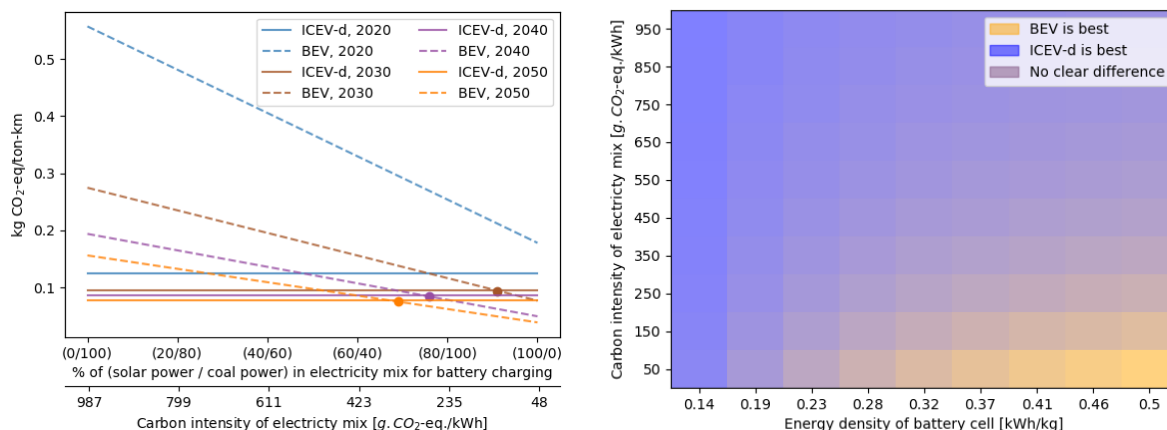
a) GHG emissions per ton-km function of gross vehicle weight, with relative difference with preceding size class, with a diesel powertrain in 2020

b) GHG emissions per ton-km as a function of range autonomy, for a 40-ton battery electric truck

399 Figure 4 GHG emissions per ton-km as a function of gross vehicle weight (left) and range autonomy (right).

400 3.3 Diesel, batteries, or fuel cells?

401 This section identifies determining parameters that can promote a certain powertrain technology over another
 402 one. Figure 5.a shows for which minimum carbon intensity level of the electricity grid 40-ton BEV trucks can
 403 compete with equivalent ICEV-d trucks on long-haul trips. In 2020, this does not seem possible regardless of
 404 how carbon-poor the electricity charging the batteries is. In 2050, as both drivetrains improve (i.e., ICEV-d
 405 drivetrains are increasingly assisted with an electric motor and the battery size of BEV reduce), the GHG
 406 intensity of the electricity still needs to be below 320 g CO₂-eq./kWh for BEV trucks to start outcompeting
 407 ICEV-d trucks. This shows that, as long as coal and natural gas power plants contribute substantially to the
 408 electricity mix, the likelihood of BEV trucks to compete with ICEV-d trucks in terms of GHG emissions on
 409 long haul applications is low. As the GHG intensity of the electricity and the battery size are two important
 410 factors determining the carbon footprint of BEV trucks, Figure 5.b shows the ratio of life cycle GHG emissions
 411 for BEV trucks over those of ICEV-d trucks for long haul operations (800 km of range autonomy), for a given
 412 combination of carbon intensity of electricity and energy density of battery cells. As this ratio tends to the favor
 413 of BEV trucks, the color of the cell tends to yellow and vice-versa. BEV trucks seem to provide an advantage
 414 over ICEV-d trucks with the condition of a minimum energy density of the battery cells of 0.3 kWh/kg
 415 combined with a maximum GHG intensity of the electricity of 100 g CO₂-eq./kWh.

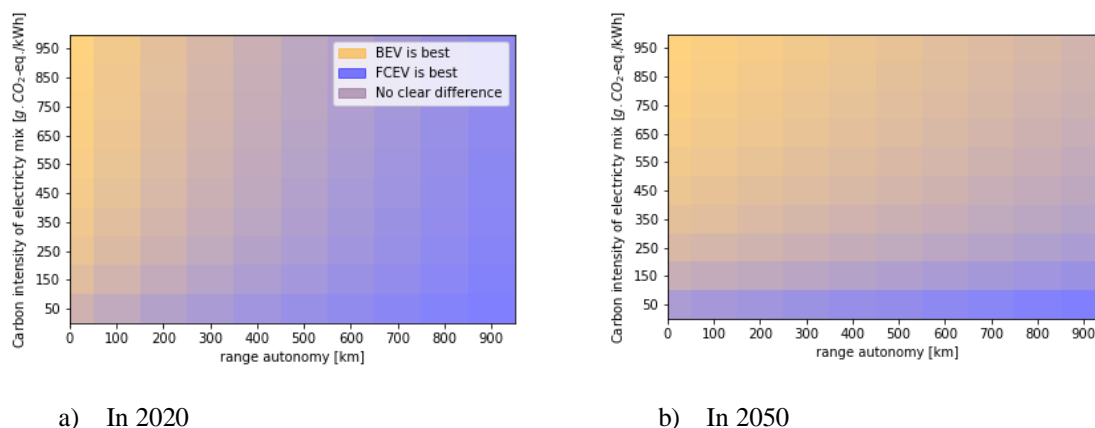


a) GHG emissions per ton-km as a function of the GHG intensity of electricity, with a range autonomy of 800 km: comparison between a 40-ton BEV and ICEV-d truck

b) GHG emissions per ton-km as a function of the GHG intensity of electricity and energy density of battery cells, with a range autonomy of 800 km: comparison between a 40-ton BEV and ICEV-d truck

416 Figure 5 Comparison between ICEV-d and BEV 40-ton trucks for long haul applications

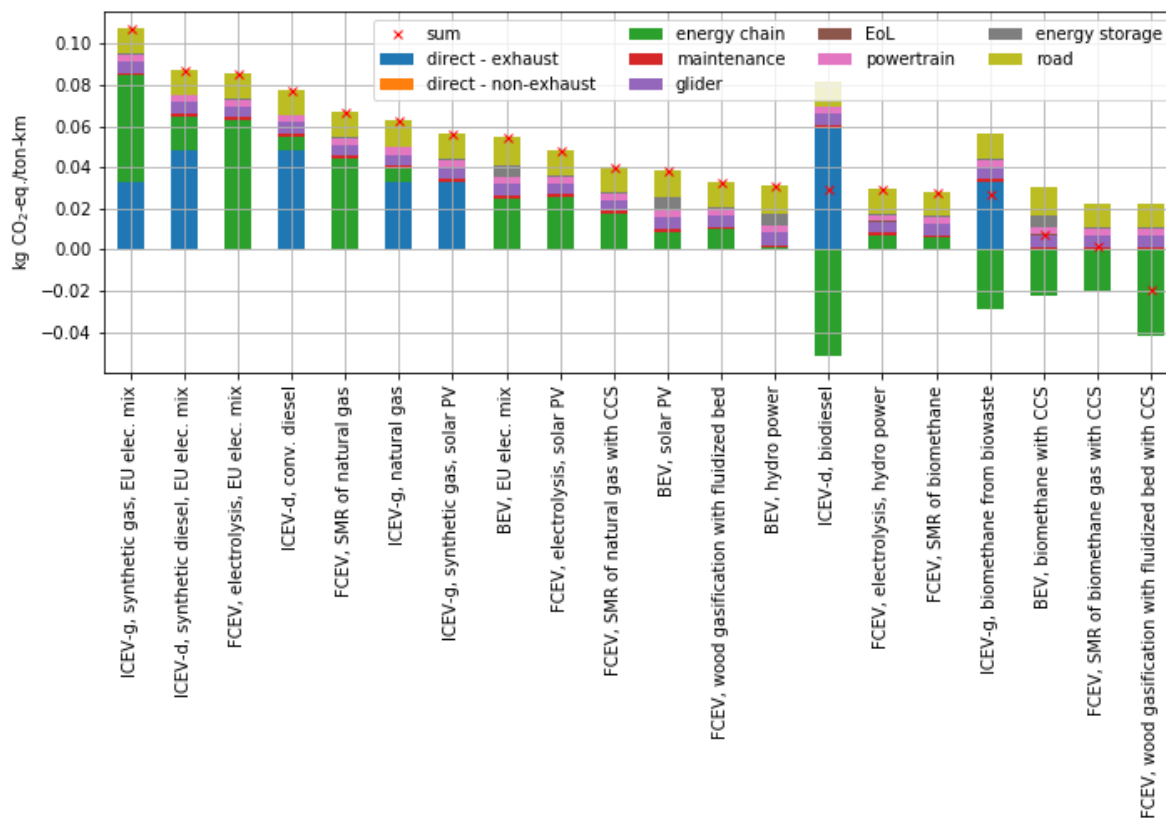
417 Regarding the comparison between BEV and FCEV trucks, besides developments in battery technology (i.e.,
 418 battery cell energy density, energy requirement for the manufacture of battery cells, etc.), improvements of the
 419 fuel cell stacks in FCEV trucks are also considered: an energy efficiency of 50% in 2020 (calibrated based on
 420 specifications from FCEV trucks manufacturers – see section 3.3 of the SI), to 58% in 2050⁵, an increase in the
 421 power area density of the cells from 0.9 W/cm² in 2020 to 1.2 W/cm² in 2050¹¹ (thereby reducing the platinum
 422 loading from 0.15 to 0.11 g Pt/kW) as well as a small reduction of the energy needed to support the balance of
 423 plant. However, no improvement has been considered regarding the production of hydrogen via electrolysis, as
 424 suggest by ⁵⁷. Figure 6 shows the ratio of life cycle GHG emissions of 40-ton BEV trucks over those of
 425 equivalent FCEV trucks, given the carbon intensity of the electricity and the required range autonomy, for 2020
 426 and 2050. In 2020, FCEV trucks have an advantage over BEV trucks for long haul usage, and this regardless of
 427 how carbon-intensive the electricity is. It still holds true in 2050, despite significant expected improvements of
 428 the battery size for BEV trucks, but only if the GHG intensity of electricity is very low (i.e., below 100 g of
 429 CO₂-eq./kWh). As the electricity becomes more carbon-intensive, the life cycle GHG emissions of BEV trucks
 430 get closer to those of FCEV trucks when the required range autonomy is high (see top right corner of Figure
 431 6.b). On the other hand, BEV trucks show lower life cycle GHG emissions when the required range autonomy is
 432 low in 2020 and 2050. This superiority is ascertained as the electricity becomes more carbon-intensive –
 433 however, past 100 g CO₂-eq./kWh, ICEV-d trucks are a better option, as seen in Figure 5.b.



434 Figure 6 Comparison of GHG emissions per ton-km between BEV and FCEV (hydrogen from electrolysis)
435 function of electricity carbon intensity and range autonomy

436 3.4 Beyond powertrains: the role of energy pathways

437 It seems however important to nuance the results, as potential future improvement may not only come from
438 efficiency gains at the vehicle level but could also be achieved through the development of emerging fuel
439 technologies. Figure 7 shows that the life cycle GHG emissions of a 40-ton diesel truck in 2050 (fourth bar to
440 the left) can be halved using low-carbon electricity directly for BEV or indirectly for FCEV trucks, as well as
441 waste biomass-based biofuels. Here, the GHG intensity considered for the European electricity mix in 2050 is
442 221 g CO₂-eq./kWh, according to the baseline projection for SSP2. Using CCS represents an option for
443 hydrogen production from natural gas and biomass. Life cycle GHG emissions close to (or even below) zero are
444 possible when using biomass-based hydrogen production with CCS, since these fuel production pathways
445 exhibit negative GHG emissions due to permanent removal of CO₂ from the atmosphere^{28,29}.



446

447 Figure 7 Per ton-km GHG emission of a 40-ton truck across different fuel pathways in 2050 (“Long haul”
 448 driving cycle, 800 km of range autonomy).

449 4 Discussion

450 Despite a comprehensive and novel approach, several limitations in this work must be acknowledged and
 451 addressed in the future:

- 452 • While the vehicle model for conventional powertrains could be calibrated against a large dataset on
 453 diesel trucks, such data are lacking for both BEV and FCEV trucks, and are limited for compressed
 454 natural gas trucks. Therefore, associated uncertainties are higher.
- 455 • Direct and indirect electrification requires establishment of additional infrastructure for battery
 456 charging which is not considered in this analysis. For hydrogen production by electrolysis, the
 457 production is assumed to occur at the fueling station, for which the necessary infrastructure is
 458 considered.
- 459 • Thanks to *rmnd_lca*, this prospective LCA considers the expected developments in the background
 460 system for the electricity sector. An analysis should be run with an ulterior version of *rmnd_lca* to

461 include expected developments in heat supply and energy-intensive industrial sectors, but also with
462 different narratives.

- 463 • While *calculator_truck* allows to quantify a complete set of midpoint indicators, the current analysis is
464 limited to impacts on climate change. Further environmental issues must be addressed, ideally applying
465 regionalized impact assessment methods to capture benefits of electric powertrains regarding human
466 health impacts in densely populated areas.

467 Limitations aside, electric powertrains seem to be the most effective option to reduce impacts on climate change
468 at large scale by 2050 – provided a “decarbonized” electricity supply. More specifically, battery electric
469 powertrains would yield most benefits in an urban context, where energy storage requirement is low and where
470 the electric motor would preserve a good efficiency despite transient loads. This relies however on expected
471 improvements that yet need to be realized, especially in terms of battery technological improvements.

472 Additionally, these improvements need to happen while keeping costs low, as they need to compete against
473 mature and well-developed diesel and natural gas-based powertrains, which, in the meanwhile, could reduce
474 their exhaust emissions by 50% through hybridization combined with biofuels. Therefore, much of the potential
475 of these emerging technologies applied to trucks is yet to be proven. Furthermore, the GHG intensity of
476 electricity is not guaranteed to be reducing at the expected pace or evenly across the globe. Fuel cell electric
477 powertrains would on the other end become a key technology for long haul transportation, where the payload
478 capacity is prioritized. They do not need to rely entirely on hydrogen from electrolysis (i.e., low-carbon
479 electricity), but can also use other low-carbon fuel production pathways, namely natural gas reforming with
480 CCS and biomass feedstock (with and without CCS). In the context of biomass-based fuels, resource limitations
481 need to be considered.

482 Finally, the environmental assessment presented here should ideally be accompanied by a cost assessment.
483 Emerging technologies must compete with mature and optimized technologies which probably have lower
484 leveled costs of ownership. In fact, hybridizing the powertrains of diesel and natural gas-powered trucks,
485 combined with the development of bio- and synthetic fuels may well provide significant reductions in terms of
486 exhaust emissions without bearing the complexity and cost of a fully electrified powertrain.

487 Acknowledgement

488 The authors thank Karin Treyer for providing inventory data for hydrogen production pathways and sharing
489 insights into the LCA of these. The authors would also like to thank Stefan Hirschberg for his valuable
490 feedback.

491 Authors information

492 Romain Sacchi joined the Technology Assessment group at the Paul Scherrer Institute in June 2019 as a
493 Postdoctoral Researcher, to contribute within the field of Life Cycle Assessment (LCA) applied to future
494 mobility technologies. Christian Bauer is working in the Technology Assessment group since 2004. His main
495 research areas are Life Cycle Assessment and sustainability assessment of current and future electricity and heat
496 supply technologies as well as conventional and innovative transport systems. Brian Cox is a scientific
497 consultant at INFRAS, where he works on transport emissions modelling and sustainable mobility.

498 Funding sources

499 This research was primarily funded by the Swiss Competence Center for Energy Research (SCCER) Efficient
500 Technologies and Systems for Mobility, financed by the Swiss Innovation Agency (Innosuisse). Further
501 contributions were provided by ACT ELEGANCY, Project No 271498, which has received funding from
502 DETEC (CH), BMWi (DE), RVO (NL), Gassnova (NO), BEIS (UK), Gassco, Equinor and Total, and is co-
503 funded by the European Commission under the Horizon 2020 programme, ACT Grant Agreement No 691712.
504 This ACT ELEGANCY project is supported by the pilot and demonstration programme of the Swiss Federal
505 Office of Energy (SFOE). In addition, this work was partially funded by the Commission for Technology and
506 Innovation in Switzerland (CTI) within the Swiss Competence Center for Energy Research in Heat and
507 Electricity Storage.

508 References

- 509 (1) Allen, M.; Babiker, M.; Chen, Y.; Taylor, M.; Tschakert Australia, P.; Waisman, H.; Warren, R.; Zhai,
510 P.; Zickfeld, K.; Zhai, P.; Pörtner, H.; Roberts, D.; Skea, J.; Shukla, P.; Pirani, A.; Moufouma-Okia, W.;
511 Péan, C.; Pidcock, R.; Connors, S.; Matthews, J.; Chen, Y.; Zhou, X.; Gomis, M.; Lonnoy, E.; Maycock,
512 T.; Tignor, M.; Waterfield, T. *Summary for Policymakers. In: Global Warming of 1.5°C. An IPCC
513 Special Report on the Impacts of Global Warming of 1.5°C above Pre-Industrial Levels and Related
514 Global Greenhouse Gas Emission Pathways, in the Context of Strengthening the Global Response To;*
515 2018.
- 516 (2) IEA. Trucks and Buses <https://www.iea.org/reports/trucks-and-buses> (accessed Aug 4, 2020).
- 517 (3) IEA. Global Energy & CO2 Status Report 2019 <https://www.iea.org/reports/global-energy-co2-status->

- 518 report-2019/emissions (accessed Aug 4, 2020).
- 519 (4) European Commission. REGULATION (EU) 2019/1242. European Commission: Brussels 2019.
- 520 (5) Cox, B.; Bauer, C.; Mendoza Beltran, A.; van Vuuren, D. P.; Mutel, C. L. Life Cycle Environmental and
521 Cost Comparison of Current and Future Passenger Cars under Different Energy Scenarios. *Appl. Energy*
522 **2020**, *269* (Cml). <https://doi.org/10.1016/j.apenergy.2020.115021>.
- 523 (6) Sacchi, R.; Bauer, C.; Cox, B.; Mutel, C. Carculator: An Open-Source Tool for Prospective
524 Environmental and Economic Life Cycle Assessment of Vehicles. When, Where and How Can Battery-
525 Electric Vehicles Help Reduce Greenhouse Gas Emissions? *Renew. Sustain. Energy Rev.* **2020**,
526 *submitted*.
- 527 (7) Bauer, C.; Hofer, J.; Althaus, H.-J.; Del Duce, A.; Simons, A. The Environmental Performance of
528 Current and Future Passenger Vehicles: Life Cycle Assessment Based on a Novel Scenario Analysis
529 Framework. *Appl. Energy* **2015**, *157*. <https://doi.org/10.1016/j.apenergy.2015.01.019>.
- 530 (8) Knobloch, F.; Hanssen, S. V.; Lam, A.; Pollitt, H.; Salas, P.; Chewpreecha, U.; Huijbregts, M. A. J.;
531 Mercure, J.-F. Net Emission Reductions from Electric Cars and Heat Pumps in 59 World Regions over
532 Time. *Nat. Sustain.* **2020**, 1–11. <https://doi.org/10.1038/s41893-020-0488-7>.
- 533 (9) Miotti, M.; Supran, G. J.; Kim, E. J.; Trancik, J. E. Personal Vehicles Evaluated against Climate Change
534 Mitigation Targets. *Environ. Sci. Technol.* **2016**, *50* (20), 10795–10804.
535 <https://doi.org/10.1021/acs.est.6b00177>.
- 536 (10) Nordelöf, A.; Messagie, M.; Tillman, A.-M.; Ljunggren Söderman, M.; Van Mierlo, J. Environmental
537 Impacts of Hybrid, Plug-in Hybrid, and Battery Electric Vehicles—What Can We Learn from Life
538 Cycle Assessment? *Int. J. Life Cycle Assess.* **2014**, *19* (11), 1866–1890. <https://doi.org/10.1007/s11367-014-0788-0>.
- 540 (11) Miotti, M.; Hofer, J.; Bauer, C. Integrated Environmental and Economic Assessment of Current and
541 Future Fuel Cell Vehicles. *Int. J. Life Cycle Assess.* **2015**, *22* (1), 94–110.
- 542 (12) Hawkins, T. R.; Singh, B.; Majeau-Bettez, G.; Strømman, A. H. Comparative Environmental Life Cycle
543 Assessment of Conventional and Electric Vehicles. *J. Ind. Ecol.* **2013**, *17* (1), 53–64.
544 <https://doi.org/10.1111/j.1530-9290.2012.00532.x>.
- 545 (13) Elgowainy, A.; Han, J.; Ward, J.; Joseck, F.; Gohlke, D.; Lindauer, A.; Ramsden, T.; Bidy, M.;
546 Alexander, M.; Barnhart, S.; Sutherland, I.; Verduzco, L.; Wallington, T. J. Current and Future United
547 States Light-Duty Vehicle Pathways: Cradle-to-Grave Lifecycle Greenhouse Gas Emissions and
548 Economic Assessment. *Environ. Sci. Technol.* **2018**, *52* (4), 2392–2399.
549 <https://doi.org/10.1021/acs.est.7b06006>.
- 550 (14) Lee, D. Y.; Thomas, V. M. Parametric Modeling Approach for Economic and Environmental Life Cycle
551 Assessment of Medium-Duty Truck Electrification. *J. Clean. Prod.* **2017**, *142*, 3300–3321.
552 <https://doi.org/10.1016/j.jclepro.2016.10.139>.
- 553 (15) Sen, B.; Ercan, T.; Tatari, O. Does a Battery-Electric Truck Make a Difference? – Life Cycle Emissions,
554 Costs, and Externality Analysis of Alternative Fuel-Powered Class 8 Heavy-Duty Trucks in the United
555 States. *J. Clean. Prod.* **2017**, *141* (2017), 110–121. <https://doi.org/10.1016/j.jclepro.2016.09.046>.
- 556 (16) Lee, D. Y.; Elgowainy, A.; Kotz, A.; Vijayagopal, R.; Marcinkoski, J. Life-Cycle Implications of
557 Hydrogen Fuel Cell Electric Vehicle Technology for Medium- and Heavy-Duty Trucks. *J. Power*
558 *Sources* **2018**, *393* (May), 217–229. <https://doi.org/10.1016/j.jpowsour.2018.05.012>.
- 559 (17) Rupp, M.; Schulze, S.; Kuperjans, I. Comparative Life Cycle Analysis of Conventional and Hybrid
560 Heavy-Duty Trucks. *World Electr. Veh. J.* **2018**, *9* (2). <https://doi.org/10.3390/wevj9020033>.
- 561 (18) Yang, L.; Hao, C.; Chai, Y. Life Cycle Assessment of Commercial Delivery Trucks: Diesel, Plug-in
562 Electric, and Battery-Swap Electric. *Sustain.* **2018**, *10* (12). <https://doi.org/10.3390/su10124547>.
- 563 (19) Sripad, S.; Viswanathan, V. Performance Metrics Required of Next-Generation Batteries to Make a
564 Practical Electric Semi Truck. *ACS Energy Letters.* 2017, pp 1669–1673.
565 <https://doi.org/10.1021/acsenergylett.7b00432>.
- 566 (20) ISO. *Environmental Management — Life Cycle Assessment — Principles and Framework*; 2006.
567 <https://doi.org/10.1136/bmj.332.7550.1107>.
- 568 (21) ISO. ISO 14044 -- Environmental Management — Life Cycle Assessment — Requirements and

- 569 Guidelines. *Iso 14044*. International Standard Organisation 2006, pp 1–54.
570 <https://doi.org/10.1007/s11367-011-0297-3>.
- 571 (22) Hill, N.; Norris, J.; Kirsch, F.; Dun, C. *Light Weighting as a Means of Improving Heavy Duty Vehicles’*
572 *Energy Efficiency and Overall CO2 Emissions Heavy Duty Vehicles Framework Contract-Service*
573 *Request 2 Executive Summary Introduction and Scope*; 2015.
- 574 (23) Wolff, S.; Seidenfus, M.; Gordon, K.; Álvarez, S.; Kalt, S.; Lienkamp, M. Scalable Life-Cycle
575 Inventory for Heavy-Duty Vehicle Production. *Sustain.* **2020**, *12* (13).
576 <https://doi.org/10.3390/su12135396>.
- 577 (24) Car2db. Car Make Model Trim Database MySQL, CSV Jan 01, 2020 — car2db.com
578 <https://car2db.com/> (accessed Jan 25, 2020).
- 579 (25) European Aluminium Association. *Aluminium in Cars - Unlocking the Light-Weighting Potential*; 2020.
- 580 (26) Dai, Q.; Kelly, J. C.; Gaines, L.; Wang, M. Life Cycle Analysis of Lithium-Ion Batteries for Automotive
581 Applications. *Batteries* **2019**, *5* (2), 48. <https://doi.org/10.3390/batteries5020048>.
- 582 (27) Ding, Y.; Cano, Z. P.; Yu, A.; Lu, J.; Chen, Z. Automotive Li-Ion Batteries: Current Status and Future
583 Perspectives. *Electrochem. Energy Rev.* **2019**, *2* (1), 1–28. <https://doi.org/10.1007/s41918-018-0022-z>.
- 584 (28) Antonini, C.; Treyer, K.; Streb, A.; van der Spek, M.; Bauer, C.; Mazzotti, M. Hydrogen Production
585 from Natural Gas and Biomethane with Carbon Capture and Storage - A Techno-Environmental
586 Analysis. *Sustain. Energy Fuels* **2020**, *4* (6), 2967–2986. <https://doi.org/10.1039/d0se00222d>.
- 587 (29) Antonini, C.; Treyer, K.; Moiola, E.; Bauer, C.; Marco, M. Hydrogen from Wood Gasification with CCS
588 - a Techno-Environmental Analysis of Production and Use as Transport Fuel (in Review). *Sustain.*
589 *Energy Fuels* **2020**.
- 590 (30) Zhang, X.; Witte, J.; Schildhauer, T.; Bauer, C. Life Cycle Assessment of Power-to-Gas with Biogas as
591 the Carbon Source. *Sustain. Energy Fuels* **2020**, *4* (3), 1427–1436. <https://doi.org/10.1039/c9se00986h>.
- 592 (31) Capros, P. EU Reference Scenario 2016. *EU Ref. Scenar. 2016* **2016**, 27. <https://doi.org/10.2833/9127>.
- 593 (32) Pappis, I.; Howells, M.; Sridharan, V.; Gardumi, A.; Ramos, E. *Energy Projections for African*
594 *Countries*; 2019. <https://doi.org/10.2760/678700>.
- 595 (33) International Energy Agency (IEA). World Energy Outlook 2017 [https://www.iea.org/reports/world-](https://www.iea.org/reports/world-energy-outlook-2017)
596 [energy-outlook-2017](https://www.iea.org/reports/world-energy-outlook-2017) (accessed Jan 26, 2020).
- 597 (34) European Commission. Vehicle Energy Consumption calculation TOol - VECTO
598 https://ec.europa.eu/clima/policies/transport/vehicles/vecto_en (accessed Sep 15, 2020).
- 599 (35) Speirs, J.; Balcombe, P.; Blomerus, P.; Stettler, M.; Achurra-Gonzalez, P.; Woo, M.; Ainalis, D.;
600 Cooper, J.; Sharafian, A.; Merida, W.; Crow, D.; Giarola, S.; Shah, N.; Brandon, N.; Hawkes, A.
601 Natural Gas Fuel and Greenhouse Gas Emissions in Trucks and Ships. *Prog. Energy* **2020**, *2* (1),
602 012002. <https://doi.org/10.1088/2516-1083/ab56af>.
- 603 (36) Transport & Environment. *20 Years of Truck Fuel Efficiency-What Progress? Methodological Note*;
604 2016.
- 605 (37) Rodriguez, F. *CO2 Standards for Heavy-Duty Vehicles in the European Union*; 2019.
- 606 (38) Meszler, D.; Delgado, O.; Rodríguez, F.; Muncrief, R. *EUROPEAN HEAVY-DUTY VEHICLES: COST-*
607 *EFFECTIVENESS OF FUEL-EFFICIENCY TECHNOLOGIES FOR LONG-HAUL TRACTOR-*
608 *TRAILERS IN THE 2025-2030 TIMEFRAME*; 2018.
- 609 (39) Spielmann, M.; Bauer, C.; Dones, R.; Scherrer, P.; Tuchschnid, V. M. *Swiss Centre for Life Cycle*
610 *Inventories A Joint Initiative of the ETH Domain and Swiss Federal Offices Transport Services*; 2007.
- 611 (40) INFRAS. Handbook Emission Factors for Road Transport version 4.1
612 <https://www.hbefa.net/e/index.html>.
- 613 (41) Xie, Y.; Posada, F.; Minjares, R. Diesel Sulfur Content Impacts on Euro VI Soot-Free Vehicles:
614 Considerations for Emerging Markets. **2020**. <https://doi.org/10.1007/s11783-016-0859-5>.
- 615 (42) United Nations. Global Sulphur Levels | UNEP - UN Environment Programme
616 <https://www.unenvironment.org/global-sulphur-levels> (accessed Sep 22, 2020).
- 617 (43) 1.A.3.b.i-iv Road transport 2019 — European Environment Agency

- 618 [https://www.eea.europa.eu/publications/emep-eea-guidebook-2019/part-b-sectoral-guidance-chapters/1-](https://www.eea.europa.eu/publications/emep-eea-guidebook-2019/part-b-sectoral-guidance-chapters/1-energy/1-a-combustion/1-a-3-b-i/view)
619 [energy/1-a-combustion/1-a-3-b-i/view](https://www.eea.europa.eu/publications/emep-eea-guidebook-2019/part-b-sectoral-guidance-chapters/1-energy/1-a-combustion/1-a-3-b-i/view) (accessed Nov 2, 2020).
- 620 (44) Eudy, L.; Post, M.; Jeffers, M. *American Fuel Cell Bus Project Evaluation: Third Report*; 2011.
- 621 (45) Kephelopoulos, S.; Paviotti, M.; Anfosso-Lédée, F. *Common Noise Assessment Methods in Europe*
622 *(CNOSSOS-EU)*; 2012.
- 623 (46) Pallas, M. A.; Bérengier, M.; Chatagnon, R.; Czuka, M.; Conter, M.; Muirhead, M. Towards a Model
624 for Electric Vehicle Noise Emission in the European Prediction Method CNOSSOS-EU. *Appl. Acoust.*
625 **2016**, *113*, 89–101. <https://doi.org/10.1016/j.apacoust.2016.06.012>.
- 626 (47) Cucurachi, S.; Schiess, S.; Froemelt, A.; Hellweg, S. Noise Footprint from Personal Land-based
627 Mobility. *J. Ind. Ecol.* **2019**, *23* (5), 1028–1038. <https://doi.org/10.1111/jiec.12837>.
- 628 (48) Dirnaichner, A.; Cox, B.; Sacchi, R.; Mutel, C. Romainsacchi/Rmnd-Lca: Coupling REMIND Output to
629 Ecoinvent LCA Databases. Github 2019.
- 630 (49) Aboumahboub, T.; Auer, C.; Bauer, N.; Baumstark, L.; Bertram, C.; Bi, S.; Dietrich, J.; Dirnaichner, A.;
631 Giannousakis, A.; Haller, M.; Hilaire, J.; Klein, D.; Koch, J.; Körner, A.; Kriegler, E.; Leimbach, M.;
632 Levesque, A.; Lorenz, A.; Luderer, G.; Ludig, S.; Lüken, M.; Malik, A.; Manger, S.; Merfort, L.;
633 Mouratiadou, I.; Pehl, M.; Pietzker, R.; Piontek, F.; Popin, L.; Rauner, S.; Rodrigues, R.; Roming, N.;
634 Rottoli, M.; Schmidt, E.; Schreyer, F.; Schultes, A.; Sörgel, B.; Strefler, J.; Ueckerdt, F. REMIND -
635 REgional Model of INvestments and Development. **2020**. <https://doi.org/10.5281/ZENODO.3730919>.
- 636 (50) Wernet, G.; Bauer, C.; Steubing, B.; Reinhard, J.; Moreno-Ruiz, E.; Weidema, B. The Ecoinvent
637 Database Version 3 (Part I): Overview and Methodology. *Int. J. Life Cycle Assess.* **2016**, *21* (9), 1218–
638 1230. <https://doi.org/10.1007/s11367-016-1087-8>.
- 639 (51) Riahi, K.; van Vuuren, D. P.; Kriegler, E.; Edmonds, J.; O'Neill, B. C.; Fujimori, S.; Bauer, N.; Calvin,
640 K.; Dellink, R.; Fricko, O.; Lutz, W.; Popp, A.; Cuaresma, J. C.; KC, S.; Leimbach, M.; Jiang, L.; Kram,
641 T.; Rao, S.; Emmerling, J.; Ebi, K.; Hasegawa, T.; Havlik, P.; Humpenöder, F.; Da Silva, L. A.; Smith,
642 S.; Stehfest, E.; Bosetti, V.; Eom, J.; Gernaat, D.; Masui, T.; Rogelj, J.; Strefler, J.; Drouet, L.; Krey, V.;
643 Luderer, G.; Harmsen, M.; Takahashi, K.; Baumstark, L.; Doelman, J. C.; Kainuma, M.; Klimont, Z.;
644 Marangoni, G.; Lotze-Campen, H.; Obersteiner, M.; Tabeau, A.; Tavoni, M. The Shared Socioeconomic
645 Pathways and Their Energy, Land Use, and Greenhouse Gas Emissions Implications: An Overview.
646 *Glob. Environ. Chang.* **2017**, *42*, 153–168. <https://doi.org/10.1016/j.gloenvcha.2016.05.009>.
- 647 (52) Goedkoop, M.; Heijungs, R.; De Schryver, A.; Struijs, J.; Van Zelm, R. *ReCiPe 2008 A Life Cycle*
648 *Impact Assessment Method Which Comprises Harmonised Category Indicators at the Midpoint and the*
649 *Endpoint Level First Edition Report I: Characterisation Mark Huijbregts 3*); 2009.
- 650 (53) Fazio, S.; Biganzioli, F.; De Laurentiis, V.; Zampori, L.; Sala, S.; Diaconu, E. *Supporting Information to*
651 *the Characterisation Factors of Recommended EF LCIA Methods*; 2018.
652 <https://doi.org/10.2760/002447>.
- 653 (54) Mutel, C. Brightway: An Open Source Framework for Life Cycle Assessment. *J. Open Source Softw.*
654 **2017**, *2* (12), 236. <https://doi.org/10.21105/joss.00236>.
- 655 (55) Pré. SimaPro | The world's leading LCA software <https://simapro.com/> (accessed Sep 17, 2020).
- 656 (56) IPCC. Climate Change 2014: Synthesis Report. Contribution of Working Groups I, II and III to the Fifth
657 Assessment Report of the Intergovernmental Panel on Climate Change. *Core Writ. Team, R.K. Pachauri*
658 *L.A. Meyer* **2014**, 151. <https://doi.org/10.1017/CBO9781107415324.004>.
- 659 (57) Schmidt, O.; Gambhir, A.; Staffell, I.; Hawkes, A.; Nelson, J.; Few, S. Future Cost and Performance of
660 Water Electrolysis: An Expert Elicitation Study. *Int. J. Hydrogen Energy* **2017**, *42* (52), 30470–30492.
661 <https://doi.org/10.1016/j.ijhydene.2017.10.045>.
- 662
- 663